약학석사 학위논문

면역 촉진을 통한
Human Cysteinyl-tRNA Synthetase의 항암 활성

Anti-tumorigenic Activity of Human Cysteinyl-tRNA Synthetase via Immune Stimulation

2018 년 2 월

서울대학교 융합과학기술대학원

분자의학 및 바이오제약학과 의약생명과학전공

한 만 규

면역 촉진을 통한

Human Cysteinyl-tRNA Synthetase의 항암 활성

Anti-tumorigenic Activity of Human Cysteinyl-tRNA Synthetase via Immune Stimulation

지도교수 김 성 훈

이 논문을 약학석사 학위논문으로 제출함

2018 년 1 월

서울대학교 융합과학기술대학원
분자의학 및 바이오제약학과 의약생명과학전공
한 만 규

한만규의 약학석사 학위논문을 인준함
2018 년 1 월

위 원 장 [illegible] (인)
부 위 원 장 김 성 훈 (인)
위 원 신 영 기 (인)

ABSTRACT

Anti-tumorigenic Activity of Human Cysteinyl-tRNA Synthetase via Immune Stimulation

Mankyu Han

Biophamaceutical Sciencs

Molecular Medicine and Biopharmaceutical Sciences

The Graduate School

Seoul National University

Cancer immunotherapy drug is getting the spotlight in cancer therapy field as a new method for treating patients in cancer. Its supportive role in immune system covers disadvantages from conventional treatments (chemotherapy, surgical resection and radiotherapy) by lowering toxicity, encouraging durability, and extending applicable types and stages of tumor. Here, we used aminoacyl-tRNA synthetases (ARSs), which are commonly known for ligating amino acids to their cognate tRNAs, as a new candidate for cancer immunotherapy. Even though its role as a housekeeping enzyme has been known, evidence on non-canonical function of ARSs is mounting and its involvement in human diseases has been discovered. We proved that cysteinyl-tRNA synthetase (CRS) has an ability to suppress tumor growth by stimulating immune responses. Through the screening using syngeneic mouse model, we confirmed that CRS could suppress the tumor growth. With the binding assay using different cell types, we observed that

recombinant CRS bound specifically to the macrophage and induced migration and TNF-α secretion of RAW 264.7 cells *in vitro*. In addition, CRS showed anti-tumorigenic activity by inducing TNF-α secretion and infiltration of macrophages into the tumor microenvironment *in vivo*. Lastly, we used various cytokines and growth factors to figure out physiological condition of CRS secretion. Interestingly, CRS was secreted from colon cancer cell line in response to TNF-α and tunicamycin (ER stress). Through this work, we concluded that secreted CRS might act as a chemokine or pro-inflammatory cytokine to stimulate immune response, there by leading to anti-tumor response.

Key words : Cysteinyl-tRNA synthetase, Immunotherapy, Macrophage, TNF-α, Chemokine, Cytokine

Student Number : 2016-26019

CONTENTS

LIST OF FIGURES

ABBREVIATION LIST

ARS: Aminoacyl-tRNA synthetase

CCK-8: Cell Counting Kit-8

CRS: Cysteinyl-tRNA synthetase

DC: Dendritic cell

ELISA: Enzyme-linked immunosorbent assay

FDA: Food and Drug Administration

KRS: Lysyl-tRNA synthetase

LPS: Lipopolysaccharide

TNF-α: Tumor necrosis factor-alpha

WRS: Tryptophanyl-tRNA synthetase

YRS: Tyrosyl-tRNA synthetase

INTRODUCTION

Cancer immunotherapy has been burgeoning since ipilimumab, anti-CTLA-4 antibody, got approved by the U.S. Food and Drug Administration (FDA) in 2011 for treating of melanoma (1). Global market of cancer immunotherapy is predicted to reach $119.4 billion in 2021 (2). Types of immunotherapy drugs are diverse, including monoclonal antibodies, checkpoint inhibitors, and cytokines. In 2017, U.S. FDA approved six cancer immunotherapy drugs, including CAR (chimeric antigen receptor) T cells therapy, anti-PD-1 antibody, and anti-PD-L1 antibody (i.e. Tisagenlecleucel, Nivolumab, Avelumab, Atezolizumab, Durvalumab, and Pembrolizumab). Cancer immunotherapy has several advantages over standard treatments known as surgery, chemotherapy, and radiation. Tumor-specific and activated immune cells could efficiently approach and eliminate tumor cells in microscopic area that surgeon cannot do. Effects of chemotherapy and radiation are commonly temporary. But long-term restraint can be possible by cancer immunotherapy because memory cells are able to subdue the recurrence of the cancer (3).

Aminoacyl-tRNA synthetases (ARSs) have been known to have diverse functions except for ligating amino acids to cognate tRNAs. In addition to canonical function, several secreted ARSs conduct many functions in tumor microenvironment, including control of angiogenesis and immune response (4, 5). Proinflammatory cytokine TNF-α induces secretion of lysyl-tRNA synthetase (KRS) from cancer cell and secreted KRS induces migration of RAW 264.7 cells (6). Tryptophanyl-tRNA synthetase (WRS) induces phagocytosis and production of

TNF-α and chemokine, following secretion from monocytes (7). Fragment of secreted tyrosyl-tRNA synthetase (YRS) induces macrophage recruitments (8). Fas ligand released from tumor cells induces secretion of glycyl-tRNA synthetase (GRS) from macrophages. And the secreted GRS has anti-tumor activity by inducing apoptosis through binding to cadherin 6 (9).

In cancer immunotherapy, syngeneic mouse model has been widely used as preclinical model to study the anti-tumorigenic effect of drug candidates (10). The immune related function of drug candidates could be effectively evaluated in the syngeneic mouse model in the presence of intact immune system. Unlike xenograft model using human cell line, cell line which is genetically syngeneic to its host is injected into the syngeneic mouse model to test or find novel cancer immunotherapy drugs (11). Furthermore, choosing which tumor cell line to transplant to the host was very important because of the distinct immunogenicity of tumor cell lines (12). Among several murine cancer cell lines, CT26 (colon cancer cell line) syngeneic mouse model showed suppression in tumor growth following treatment of both anti-CTLA4 and anti-PD-L1 monoclonal antibodies which are known as immune-checkpoint inhibitors. However, 4T1 (breast cancer cell line) syngeneic mouse model did not show any inhibition in tumor growth by the administration of anti-CTLA4 and anti-PD-L1 monoclonal antibodies (10).

In this study, we found that CRS has anti-tumorigenic activity by stimulating immune response. Syngeneic mouse model was used to screen a novel anti-tumorigenic effect of ARSs through activating immune response. Among several purified ARSs, CRS-treated mice showed a tumor regression compared to control mice. Through the binding assay, migration assay, and ELISA, we

confirmed that CRS bound to the RAW 264.7 cells and induced migration and TNF-α secretion of RAW 264.7 cells *in vitro*. In addition, CRS induced TNF-α secretion and infiltration of macrophages into the tumor microenvironment *in vivo*. These results suggest that CRS has anti-tumorigenic activity by acting as a pro-inflammatory cytokine or chemokine to stimulate immune response.

MATERIALS AND METHODS

Cell culture and materials

CT26 cells were purchased from KCLB (Korean Cell Line Bank). HCT116 cells were cultured in RPMI-1640 medium (HyClone, Logan, UT). CT26 and 4T1 cells were cultured in Dulbecco's modified Eagle's medium (DMEM, HyClone). Every cells were grown with 10% fetal bovine serum (FBS, HyClone) and 1% penicillin and streptomycin (HyClone) at 37℃ in a 5% CO_2 incubator.

ARSs secretion test

HCT116 cells were transfected with each ARS and empty vector using Lipofectamine 2000 (Invitrogen, Carlsbad, CA). The transfected HCT116 cells were then cultured in RPMI-1640 with 10% FBS and 1% antibiotics to 60% confluency. Serum free RPMI were added for 24 hours after washing the cells. The media were centrifuged at 500 g for 10 minutes. The supernatants were further centrifuged at 10,000 g for 30 minutes. Proteins were precipitated with 12% TCA at 4℃ for 12 hours. After centrifuged at 18,000 g for 15 minutes, pellets were neutralized with 100 mM Hepes (pH 8.0). Proteins were separated using SDS-PAGE and immunoblotted using anti-strep-tag antibody (IBA Lifesciences, Goettingne, Germany).

Preparation of ARSs

The cDNA for human cytosolic ARSs were subcloned into pET28a and

expressed in *Escherichia coli* BL21. His-tagged ARSs were purified using Ni-NTA resin. Eluted solution was dialyzed in 15% glycerol in PBS and filtered through Acrodisc Units with Mustang E membrane (0.2 μm, Pall Corporation, Port Washington, NY). Coomassie Blue staining (Sigma) and immunoblotting using His-probe antibody (Santacruz, Dallas, TX) were done to confirm the purity and expression of ARSs.

Syngeneic mouse model

Syngeneic mouse experiments were performed in accordance with Institutional Animal Care and Use Committee guidelines at WOOJEONGBSC. 5 x 10^5 CT26 and 4T1 cells were injected into the right flank of 6 week old BALB/c female mice. When the size of the tumor reached 50 mm^3, saline or 10 mg/kg body weight ARS proteins were intraperitoneally administered at day 7, day 8, and day 9 after tumor implantation. Tumor volume and body weight were measured every 2 days (Tumor volume = length x $width^2$ x 0.52). Mice were sacrificed at day 21 and the tumor weights were measured.

For the validation experiment, saline or 10 mg/kg body weight CRS were intraperitoneally administered after tumor size reached 50 mm^3. Experiment schedule was same as previous syngeneic mouse experiment except for checking the survival. Mice were not sacrificed at day 21 to evaluate survival rate of CRS-treated mice. Mice with tumor volume below 1,500 mm^3 defined as survived.

Cell viability assay

CT26 or 4T1 cells were seeded at a density of 5 x 10^3 cells/well into 96

well plate for 24 hours in DMEM containing 10% FBS and 1% antibiotics. Proteins were treated with 100 μl serum free media and incubated for additional 24 hours. Cell viability was evaluated using Cell Counting Kit-8 (CCK-8) assay (Dojindo Laboratories, Kumamoto, Japan). After 10 μl of CCK-8 reagent was added to each well, cells were incubated for 1 hour and the optical density was measured at 450 nm using microplate reader (TECAN, Mannedorf, Swiss).

Flow cytometry

5 x 10^5 CT26 cells were injected into the right flank of 6 week old BALB/c female mice. After treatment of 10 mpk CRS at day 7, day 8, and day 9, mice were sacrificed at day 13 for FACS analysis. Spleen and tumor tissue were obtained from each mouse. After using MACS machine (Miltenyi Biotec, Bergisch Gladbach, Germany) following manufacturer's instructions, single cells were obtained from tumor tissue and then cell suspensions were further filtered using 70 μm strainer. Cells were stained with CD4, CD8, CD69, CD11b, F4/80, MHC II, and CD11c antibodies (eBioscience, San Diego, CA). All the isotypes that matched to each conjugated antibodies were used for the experiment. Staining was conducted for 30 minutes in 4℃ and then cells were washed, fixed, and analyzed using FACS ARIA III (BD Biosciences, Franklin Lakes, NJ). Spleen was mashed and passed through 70 μm strainer to remove lipids and cell clumps. CD4, CD8, and CD69 antibodies were used for staining and further steps were performed as mentioned above. Data were analyzed using FlowJo software.

RT-qPCR (Quantitative reverse transcription PCR)

RAW 264.7 cells seeded and incubated for 12 hours prior to experiments. Then, cells were starved in serum free RPMI-1640 medium for 2 hours and

incubated with different recombinant proteins for 4 hours. After washing with PBS, total RNAs were extracted by using GeneJET RNA Purification Kit (Thermo Fisher Scientific, Waltham, MA) and 1 μg of RNA was used for cDNA synthesis according to manufacturer's instructions (Thermo Fisher Scientific). RT-qPCR was carried out on an ABI 7500 instrument (Life Technologies, Carlsbad, CA) with 2 μl of cDNA template, SYBR green Master MIX with ROX solution (Thermo Fisher Scientific), and 0.3 μM of forward and reverse primers. For the mouse sample, RNA were extracted from tumor tissue and the further steps are performed as mentioned above. Primer sequences used for RT-qPCR are shown below.

Prf1 Forward : 5′- GATGTGAACCCTAGGCCAGA -3′

Prf1 Reverse : 5′- GGTTTTTGTACCAGGCGAAA -3′

Ifnγ Forward : 5′- AAGTGGCATAGATGTGGAAG -3′

Ifnγ Reverse : 5′- GAATGCATCCTTTTTCGCCT -3′

Tnfα Forward: 5′- CTCAAAATTCGAGTGACAAGCCTG -3′

Tnfα Reverse: 5′- ATCGGCTGGCACCACTAGTT -3′

Il10 Forward: 5′- AGACTTTCTTTCAAACAAAGGA-3′

Il10 Reverse: 5′- ATCGATGACAGCGCCTCAG -3′

iNOS Forward: 5′- CAGCTGGGCTGTACAAACCTT -3′

iNOS Reverse: 5′- CATTGGAAGTGAAGCGTTTCG -3′

Il6 Forward: 5′- ACCACGGCCTTCCCTACTTC -3′

Il6 Reverse: 5′- CTCATTTCCACGATTTCCCAG -3′

Il1β Forward: 5′- TTGAAGAAGAGCCCATCCTCTG -3′

Il1β Reverse: 5′- GATCCACACTCTCCAGCTGC -3′

Determination of MHCII and CD206 expression levels from tissue samples

5 x 10^5 of CT26 cells were injected subcutaneously into the right flank of BALB/c mice 7 days before CRS treatment. After tumor sizes reached approximately 40 mm^3, saline and 10 mpk of CRS are injected intraperitoneally at day 7, day 8, and day 9. At day 20, 3 mice of each group were sacrificed and tumor tissues from each mouse were obtained. Tissues were then washed with PBS and followed by fixation step with 4% PFA solution. After, paraffin blocks were successfully made by WOOJUNGBSC. Tissues were then incubated in xylene for 5 minutes, for 3 times. After immersing tissues in ethanol twice for 5 minutes, 90, 80, and 70% ethanol were used for 5 minutes in a sequential manner. Finally, tissues were washed with distilled water (DW). Next, tissues were treated with 0.3% hydrogen peroxide for 15 minutes and washed with DW. The antigens in the tissues were retrieved from the tissues in citrate buffer (pH 6.0) using microwave and washed with DW and then PBS. Then, tissues were blocked with PBS-T containing 4% BSA and washed with PBS-T. After tissues were incubated with anti-MHCII and CD206 antibodies (Abcam, Cambridge, UK) for 1 hour with manufacturer's recommended dilution factor, tissues were washed with PBS-T for 5 minutes, 3 times each. Then, horseradish peroxidase labeled poly anti-rabbit, and mouse secondary antibody were incubated for 1 hour at room temperature. Finally, blocks were washed by PBS-T three times for 5 minutes. Then, 1 ml of DAB substrate buffer was treated and chromogen 20 μl and washed with tap water. The tissues were stained with Mayer's hematoxylin and then washed. After dehydration, the expression level of MHCII and CD206 were captured using 40x microscopy.

Immunofluorescence

CT26, Daudi, and, Jurkat cells were seeded on 9 x 9 mm cover slip (Bellco Glass Inc., Vineland, NJ) in the 6 well plate and were treated with BSA and CRS for 1 hour. Cells were fixed with 4% paraformaldehyde for 10 minutes at room temperature. Cells were washed with PBS 3 times and blocked with CAS-block (Life Technology) for 10 minutes. After washed with PBS, cells were stained with DAPI (Sigma-Aldrich) for 5 minutes and washed with PBS 5 times. Then cells were mounted with mounting solution (Biomeda, Foster City, CA) on Micro Slides (Leica, Wetzlar, Germany) and cell binding was evaluated using confocal fluorescence microscopy (Nikon Instruments, Tokyo, Japan).

Cell migration assay

RAW 264.7 cell migration was evaluated with 6.5 mm Transwell® with 5.0 μm pore size (Corning, Kennebunk, ME). 10 μg/ml collagen type I (Gibco, Grand Island, NY) in PBS was coated on the underside of transwell membrane and the membrane was dried for 2 hours. 2 x 10^5 RAW 264.7 cells in serum free DMEM were seeded into each upper well. 100 nM ARSs were added to lower wells. Cells were incubated for 8 hours at 37℃ in a 5% CO_2 incubator to migrate to the underside of the porous membrane. Cells were washed with PBS twice and fixed with 70% methanol in PBS for 30 minutes at room temperature. Cells were then washed with PBS twice and stained with Hematoxylin (Sigma, St. Louis, MO) for 20 minutes at room temperature. Cells were then washed with deionized water twice and non-migrated cells were removed from the upper side of the membrane using a cotton swab. The membrane was cut out from insert and mounted. Three random images were taken by the microscope (x 20).

TNF-α secretion assay

RAW 264.7 cells were seeded into 12 well plate and 100 nM ARSs were treated for 4 hours. The media were collected and centrifuged at 3,000 g for 5 minutes. The secreted TNF-α and IL-10 were evaluated using mouse TNF-α ELISA kit (BD Bioscience) according to manufacturer's instructions.

RESULTS

CRS induces tumor regression in CT26 bearing mice, not in 4T1 bearing mice

Before we started screening of novel anti- or pro-tumor immunotherapy candidates *in vivo*, we checked the secretion of ARSs from HCT116 colon cancer cell lines which were transfected with each ARS and empty vector (Fig 1A). Several ARSs were secreted from HCT116 cells including cysteinyl-, lysyl-, and tyrosyl-tRNA synthetase. Gram-negative bacterial endotoxin, lipopolysaccharide(LPS), level in the purified ARS proteins were checked using LAL(Limulus Amebocyte Lysate) test (Fig 1B-C).

We analyzed the *in vivo* effect of six ARSs (cysteinyl-, glycyl-, histidyl-, lysyl-, threonyl- and tyrosyl-tRNA synthetase; CRS, GRS, HRS, KRS, TRS and YRS respectively) in syngeneic mouse model using CT26 (murine colon cancer) and 4T1 (murine breast cancer) cell line. Immune checkpoint inhibitor, anti-CTLA-4 antibody, was reported that it enhanced the survival in CT26 syngeneic mouse model, but not in 4T1 mouse model (13, 14). So we performed our *in vivo* screening using both responding (CT26) and non-responding (4T1) mouse model. CT26 and 4T1 cells were injected into the right flank of BALB/c mice by subcutaneous injection. Tumors were grown until the average tumor volume reached 50 mm^3. Saline or 10 mg/kg ARS were administered by intraperitoneal injection at day 7, day 8, and day 9. Tumor volume and body weight were measured every 2 days and the mice were sacrificed at day 21 after tumor implantation. In the highly immunogenic CT26 mouse model, tumor mass of YRS-, CRS-, and KRS-injected group decreased by 56%, 44%, and 52% respectively

compared to control group (Fig. 2E). But there were no significant changes in tumor mass in the 4T1 mouse model (Fig. 2F). In addition, there was no significant toxicity caused by the injection of ARSs both in two mouse models (data not shown). And we further confirmed the *in vivo* anti-tumor phenotype by the injection of CRS. The tumor volume of CRS-treated mice was decreased by 70% at day 21 compared to non-treated mice (Fig. 3A). Moreover, the treatment of CRS enhanced survival of the CT26 bearing mice (Fig. 3B). ARSs used in mouse experiments had no cytotoxic effect on CT26 and 4T1 cells (Fig. 3C-D). From this result, we could consider that immune system was related to this tumor regression phenotype of CRS-treated mice.

Stimulation of immune response by intraperitoneal injection of CRS in mice

The expression of CD40 by $CD11b^+$ $F4/80^+$ MHC II^+ macrophages increased in the CRS-treated mouse tumor tissue compared to control (Fig. 4A). CD40 is a surface protein on antigen presenting cells whose ligand is primarily expressed by activated T cells. Binding of CD40 to CD40L (CD154) results in activation of macrophages (15). Furthermore, activation of CD4 and CD8 T cells were analyzed using splenic lymphocytes. As a result, we could confirm that CRS induced activation of CD4 and CD8 T cells (Fig. 4B).

To check the innate and adaptive immune response and infiltration of immune cells in the tumor microenvironment, extracted tumor tissues from CT26 syngeneic mice model were analyzed by RT-qPCR and Immunohistochemistry (IHC). Interestingly, mRNA levels of several genes related to innate (Il6, Il1β, Tnfα)

and adaptive (Prf1, Ifnγ) response were higher in the CRS-injected mice compared to control mice. This result indicates that both innate and adaptive immune cells could be related in this tumor regression phenotype (Fig. 4C). Infiltration of anti-tumor M1 macrophages into the tumor microenvironment increased in CRS-treated mice. However, infiltration of pro-tumor M2 macrophage decreased by the injection of CRS (Fig. 4D). Because this result gives the information about immune response and infiltration only at the time point we sacrificed the mice, further experiments will be needed to analyze immune response and infiltration over time after tumor implantation.

CRS binds to RAW 264.7 cells, not to Daudi and Jurkat cells *in vitro*.

Because various immune cells could be related to the anti-tumor response caused by the injection of CRS, binding of CRS to macrophages, T cells, and B cells was tested through and Flow cytometry and immunofluorescence (IF). CRS binds to RAW 264.7 cells, but not to Jurkat and Daudi cells (Fig. 5A-B). Thus, we consider that direct binding partner of CRS is macrophages although CRS could show the anti-tumorigenic effect by indirectly making an impact on T cells through macrophages.

CRS induces migration and secretion of proinflammatory cytokine TNF-α in RAW 264.7 cells.

To investigate inflammatory effect of CRS on macrophages, we checked

TNF-α secretion from RAW 264.7 cells using ELISA. TNF-α secretion was induced in response to 100 nM CRS (Fig. 6A). We further investigate types of macrophage induced by CRS between anti-tumor M1 macrophage and pro-tumor M2 macrophage. mRNA level of M1 marker, iNOS (inducible nitric oxide synthase), was upregulated in response to 100 nM CRS (Fig. 6B). To confirm the possibility that CRS could act as chemokine for macrophages, migration of RAW 264.7 cells was evaluated using Transwell migration assay. The migration of RAW 264.7 cells was triggered by CRS compared to control (Fig. 6C). To sum up those results from *in vitro* studies using RAW 264.7 cells, CRS induces migration as well as TNF-α secretion of RAW 264.7 cells.

TNF-α and tunicamycin induces secretion of CRS from colon cancer cell line.

We investigated which signal induces the secretion of CRS from colon cancer cells. Among various cytokines and growth factors, CRS was secreted from HCT116 cells in a dose- and time-dependent manner in response to TNF-α and tunicamycin (Fig. 7A-B). Tunicamycin is a commonly known as ER stress inducer through unfolded protein response (16). To sum up those results from *in vitro* study, we consider that CRS is secreted when TNF-α and ER stress signal were transduced. And the secreted CRS could mediate anti-tumor response by acting as chemokines or inducing proinflammatory cytokines production of macrophages.

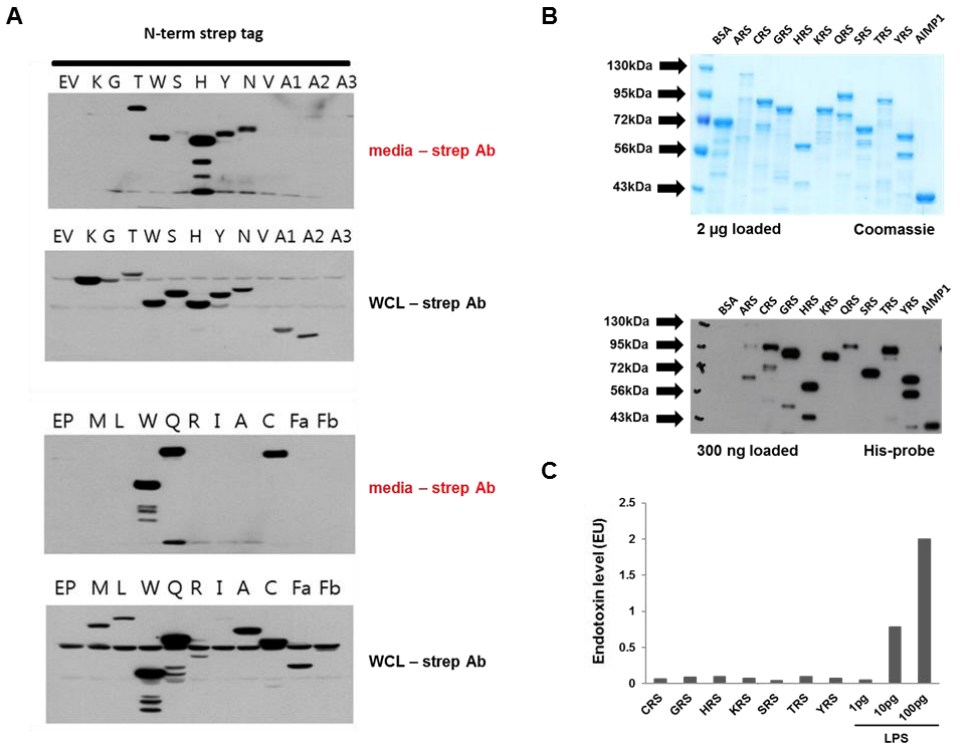

Figure 1. Purification of secreted ARSs

(A) Secretion of ARSs was evaluated in HCT116 colon cancer cell using transfection. pEXPR-IBA105 and pEXPR-IBA103(data not shown) were used to transiently express each ARS proteins. Cell lysates and secreted proteins were analyzed by SDS-PAGE and immunoblotting.

(B) ARS proteins were purified using affinity chromatography. Ni-NTA lesin was used to purify both N- and C-term His-tagged ARSs.

(C) Endotoxin levels of purified ARSs were evaluated using LAL(Limulus Amebocyte Lysate) test. LPS (lipopolysaccharide) was used as positive control.

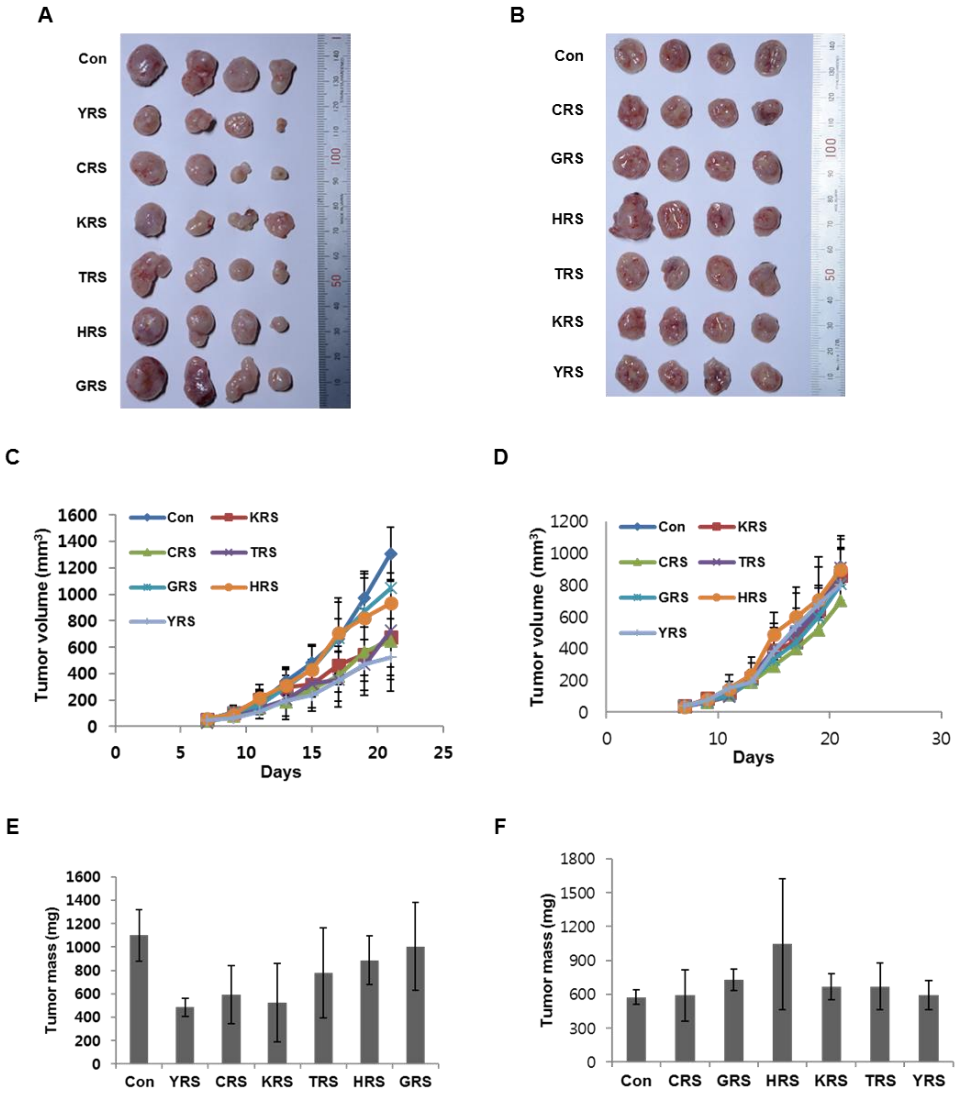

Figure 2. *In vivo* effect of ARSs on CT26 and 4T1 tumor bearing mice

(A, B) Photograph of CT26(A) and 4T1(B) tumor bearing mice. Saline and 10 mg/kg body weight ARSs were intraperitoneally injected at day 7, day 8, and day 9 after tumor implantation.

(C, D) Tumor volume of CT26(A) and 4T1(B) tumor bearing mice. CT26 and 4T1 cells (5 x 10^5 cells) were injected into the BALB/c mice by subcutaneous injection. Tumor volume was measured every 2 days after average tumor size reached 50 mm^3 (Tumor volume = length x $width^2$ x 0.52).

(E, F) Tumor mass of CT26(A) and 4T1(B) tumor bearing mice. Tumor mass was measured at day 21.

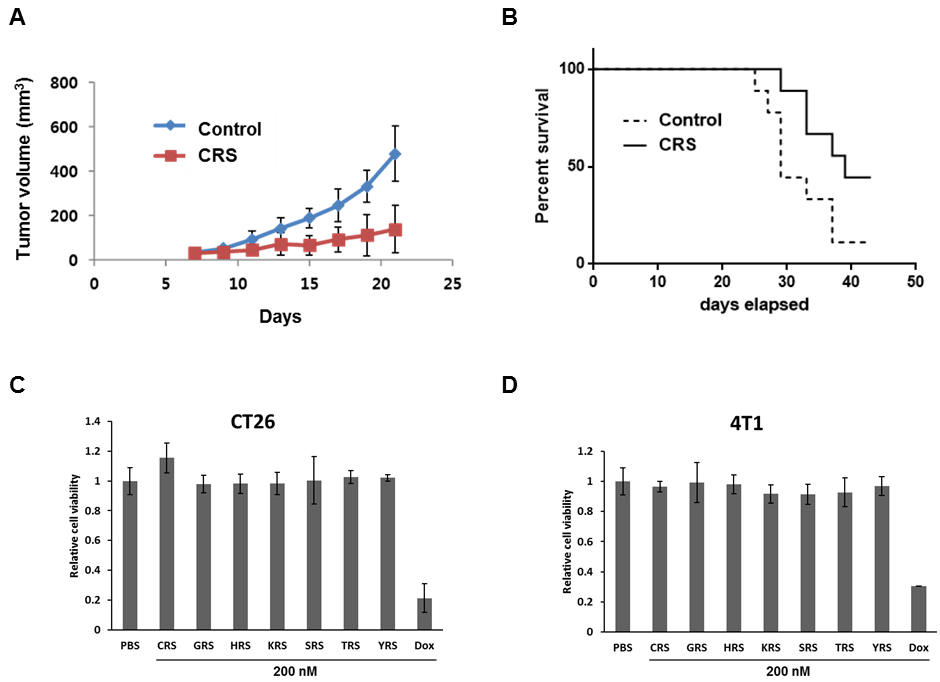

Figure 3. Validation of tumor regression effect of CRS on CT26 tumor bearing mice

(A) CT26 cells (5 x 10^5 cells) were injected into the BALB/c mice by subcutaneous injection. Saline and 10 mpk CRS were treated at day 7, day 8, and day9 after tumor implantation. Tumor volume was measured every 2 days after average tumor size reached 50 mm^3 (Tumor volume = length x $width^2$ x 0.52).

(B) Survival curve of the CT26 tumor bearing mice. Survival was defined as mouse with tumor volume < 1500 mm^3.

(C, D) Effect of ARSs on cell viability was evaluated using CT26(C) and 4T1(D) cells.

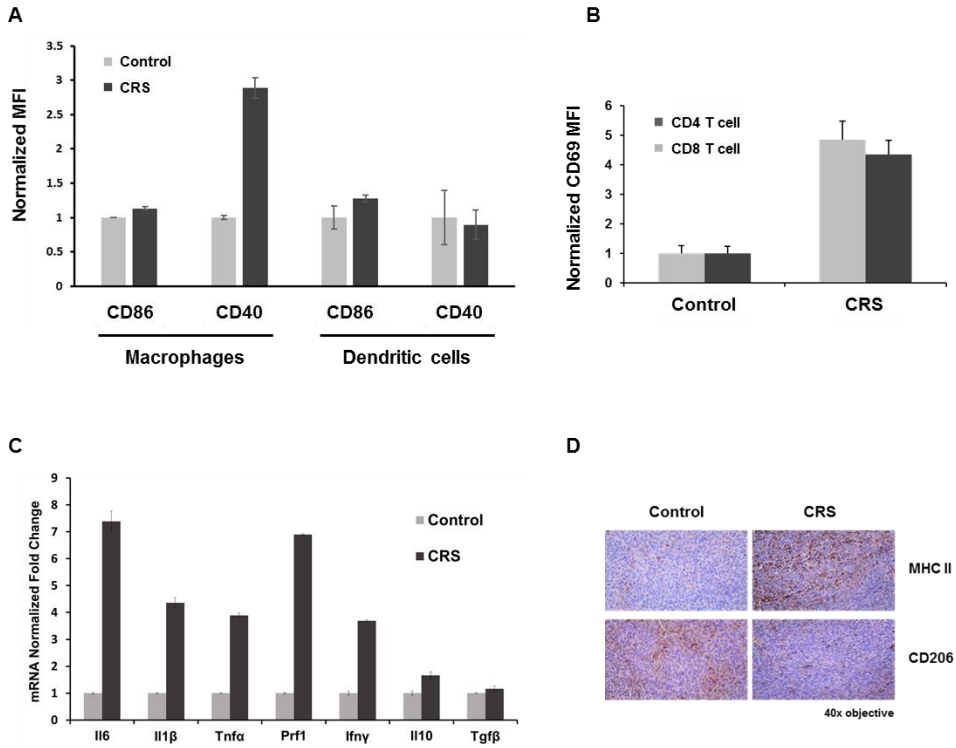

Figure 4. Stimulation of immune response by intraperitoneal injection of CRS in mice

(A) The activation markers of infiltrated macrophage (CD11b+, F4/80+, MHC II+) and dendritic cells (CD11b+, CD11c+, MHC II+), CD40 and CD86, are shown. Activation of macrophages and DCs by CRS treatment are normalized to those of control.

(B) Splenic lymphocytes were analyzed by Flow cytometry after CRS treatment. Activation of CD4 and CD8 T cells are analyzed using CD69 antibody. Activation of CD4 and CD8 T cells by CRS treatment are normalized to those of control.

(C) Changes in the tumor microenvironment by the injection of CRS. mRNA level of diverse cytokines from immune cells was evaluated using RT-qPCR. Tumor tissues were extracted from CT26 tumor bearing mice.

(D) Immunohistochemistry (IHC) staining of mouse CT26 tumor sections was performed with anti-CD206 and anti-MHCII antibodies to detect immune cell infiltration (M1 macrophage and M2 macrophage respectively).

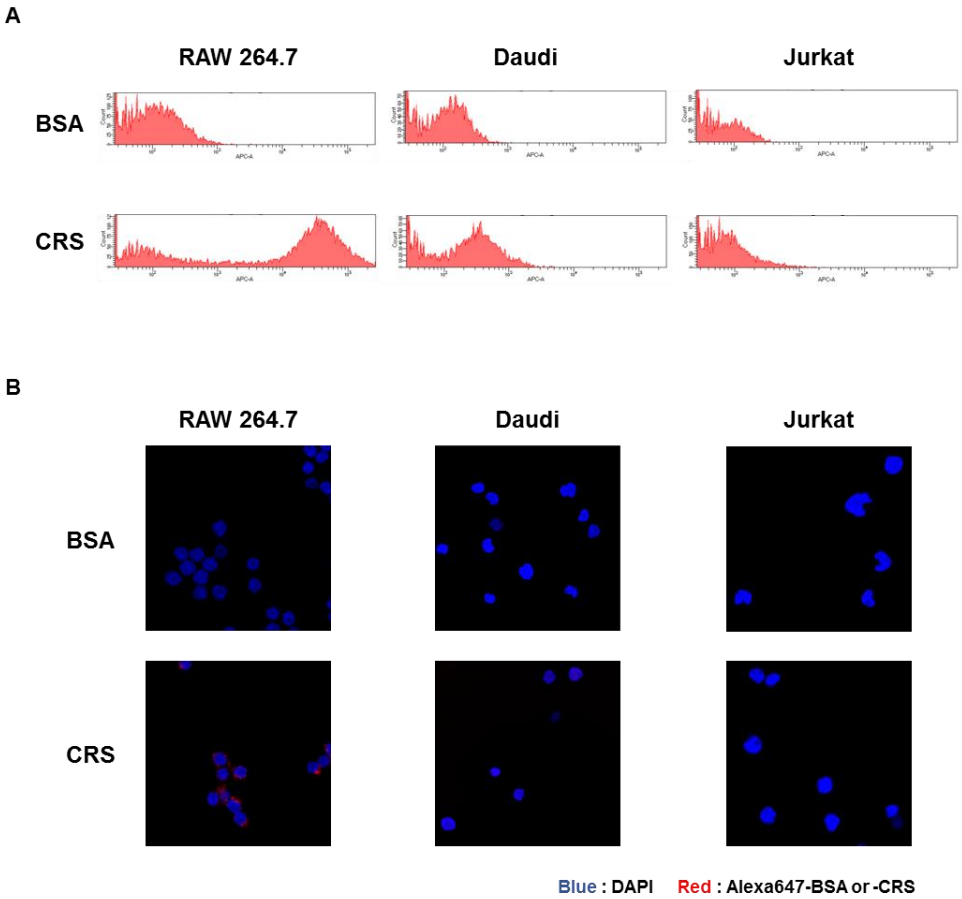

Figure 5. CRS binds to RAW 264.7 cells, not to Daudi and Jurkat cells *in vitro*

(A) Binding of CRS to RAW 264.7, Daudi, and Jurkat cells was tested using Flow cytometry. BSA and CRS were labeled with Alexa 647 NHS ester.

(B) Binding of CRS to RAW 264.7, Daudi, and Jurkat cells was evaluated using immunofluorescence (IF) staining. BSA and CRS were labeled with Alexa 647 NHS ester (red fluorescence).

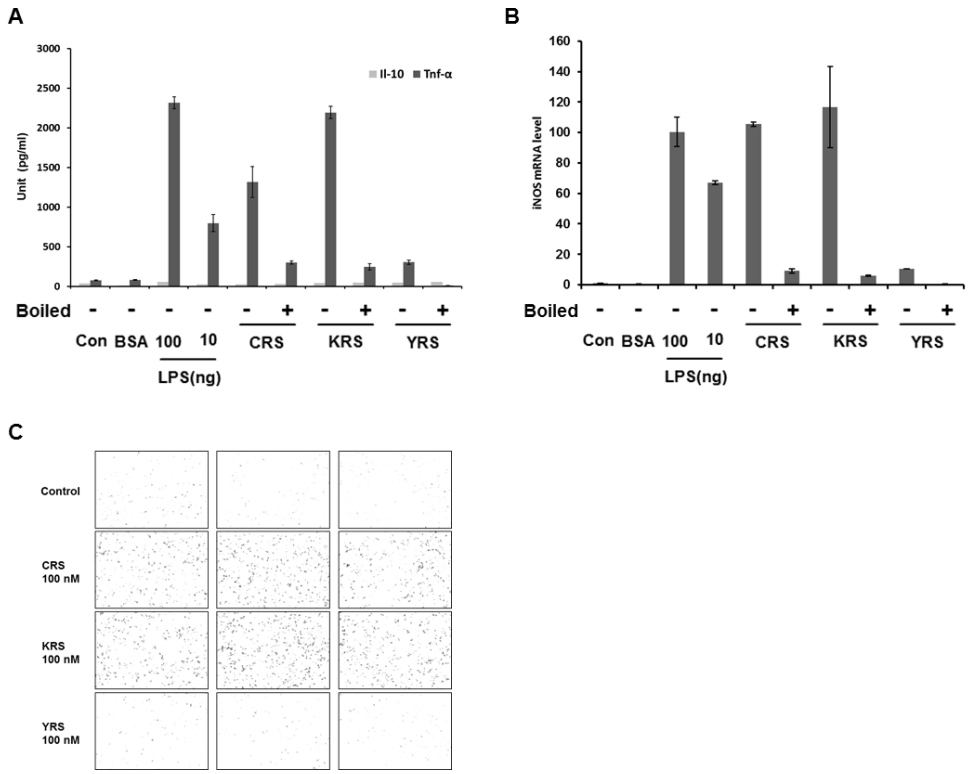

Figure 6. CRS induces migration and secretion of proinflammatory cytokine TNF-α in RAW 264.7 cells

(A) IL-10 and TNF-α secretion from RAW 264.7 cells was evaluated using ELISA. PBS and 100 nM ARSs were treated for 4 hours. LPS was used as positive control.

(B) iNOS (inducible nitric oxide synthase) mRNA level of RAW 264.7 cells was evaluated using RT-qPCR. PBS and 100 nM ARSs were treated for 4 hours. LPS was used as positive control.

(C) Migration of RAW 264.7 cells was evaluated using Transwell migration assay. RAW 264.7 cells (2 x 10^5 cells/well) were seeded in the upper wells of transwell chamber coated with collagen type 1 from rat tail. PBS and 100 nM ARSs were added in the lower wells and treated for 8 hours.

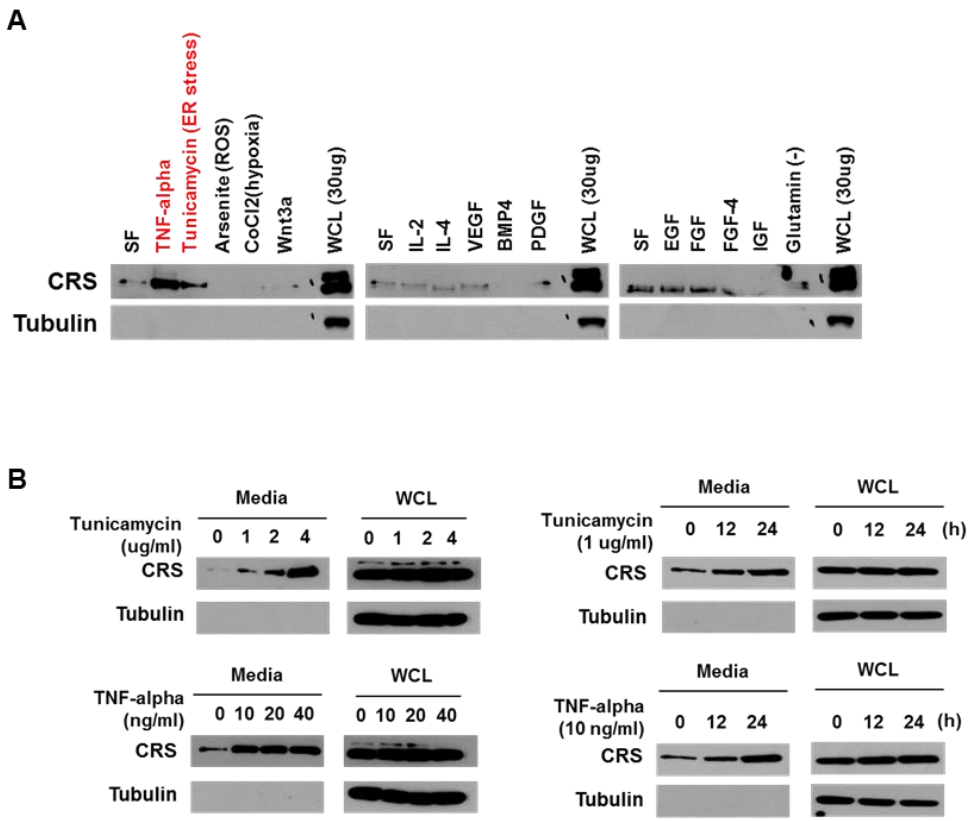

Figure 7. Secretion of CRS is dependent on TNF-α and tunicamycin (ER stress)

(A) TNF-α and tunicamycin induced secretion of CRS from HCT116 cells. Various cytokines and growth factors were treated.

(B) In response to TNF-α and tunicamycin, CRS was secreted from HCT116 cells in a time- and dose-dependent manner.

DISCUSSION

Among several ARSs secreted from HCT116 cells, purified CRS suppressed the tumor growth when it was treated to the CT26 tumor bearing mice (Fig. 1, 2). Because there was no cytotoxic effect of CRS on CT26 cells *in vitro* (Fig. 3), we could consider that the tumor suppressive phenotype of CRS-treated mice was the result of the intervention by the intact immune system of syngeneic mouse model. As we expected, macrophage and T cells were activated in the CRS-treated mice compared to control mice. Furthermore, mRNA level of various cytokines from immune cells and the infiltration of anti-tumor M1 macrophage increased in the CRS-treated mice (Fig. 4). However, further validation about the effect of some of those cytokines in tumor microenvironment should be conducted because ambivalent characteristics of those cytokines between pro- and anti-imflammation have been reported (17, 18).

CRS has been shown to have anti-tumor effect through the activation of macrophages (Fig 4, 6). In addition to its effect on macrophages, CRS induced activation and responses of adaptive immune system *in vivo* (Fig. 4). So the effect of CRS on other types of immune cells should be further investigated. Anti-tumorigenic activity of CRS should be evaluated using T cell-deficient mice (BALB/c nu/nu) to confirm the intervention of T cells of adaptive immune system. Although CRS did not bind to Jurkat cells in flow cytometry and IF analysis, *in vitro* (Fig. 5), further validation is needed using other cell lines belonging to adaptive immune system. To verify this *in vitro* results of CRS binding, *in vivo* cell binding assay should be conducted using flow cytometry. After fluorescently

labeled CRS is injected into the mice through the tail vein, binding of CRS to granulocytes, monocytes, T cells, and B cells should be analyzed following blood collection.

We found some clues about the condition related to the secretion of CRS from the cancer cells through this research using colon cancer cell lines. CRS was secreted from HCT116 cells in response to TNF-α and Tunicamycin (ER stress) (Fig. 7). Because some other ARSs were secreted from cancer cells or endothelial cells upon TNF-α, difference between CRS and other ARSs that are secreted from cancer cell in response to same signals should be investigated (6, 19). We consider that there will be a distinct mechanism of CRS secretion. To find out unique secretion mechanism of CRS, diverse cell types (cancer, immune, endothelial, and fibroblast cell) should be tried out and unique signals that result in the secretion of CRS without other ARSs should be further investigated.

Cancer immunotherapy has been highlighted with regard to inhibiting suppression of T cells. Although cancer immunotherapy drugs usually target T cells, many therapeutic strategies aiming at macrophages are going through clinical trials (20). Furthermore, importance of tumor-associated macrophages (TAMs) is highlighted because it was deeply related with conventional immunotherapy drug. For instance, PD1 inhibition induced TAM-related tumor regression in T cell-deficient mice because TAMs which express PD1 on their surface showed pro-tumorigenic M2 properties (21). Moreover, targeting macrophages would be a good strategy for developing immunotherapy drug because it could be further utilized with the conventional T cell-targeting drugs as a concept of combitherapy. In this respect, macrophage-targeting CRS has a potential to be developed as a novel

immunotherapy drug.

EGFR and CXC chemokine receptor have been developed as peptide to treat cancer by using their immunogenic properties. (22, 23) To develop CRS as therapeutic peptide, active site of CRS should be identified. Anti-tumorigenic activity of CRS fragments that reserve every pre-existing domain (i.e. catalytic domain, UNE-C1, and UNE-C2 domain) should be validated. It will be a big benefit for further development if we found shorter peptide sustaining the activity and stability of full length CRS. Moreover, various routes of CRS administration should be tested because we have administrated CRS only by intraperitoneal injection in our mouse experiments.

In this study, we confirmed the anti-tumorigenic activity of CRS by stimulating immune response related to macrophages. Even if the detail mechanism of action should be further defined, it is worth noting that we suggested a possible approach to screen and develop anti-cancer immunotherapy drug targeting macrophages by discovering novel functions of CRS.

REFERENCES

1. Hoos, A. (2016). Development of immuno-oncology drugs from CTLA4 to PD1 to the next generations. *Nature reviews Drug discovery*, 15(4), 235-247..
2. MARKETS AND MARKETS (2017). Cancer Immunotherapy Market worth 119.39 Billion USD by 2021. Retrieved from https://www.marketsandmarkets.com/PressReleases/cancer-immunotherapy.asp
3. Dimberu, P. M., & Leonhardt, R. M. (2011). Cancer immunotherapy takes a multi-faceted approach to kick the immune system into gear. *The Yale journal of biology and medicine*, 84(4), 371.
4. Guo, M., Yang, X. L., & Schimmel, P. (2010). New functions of tRNA synthetases beyond translation. *Nature reviews. Molecular cell biology*, 11(9), 668.
5. Kim, S., You, S., & Hwang, D. (2011). Aminoacyl-tRNA synthetases and tumorigenesis: more than housekeeping. *Nature Reviews Cancer*, 11(10).
6. Park, S. G., Kim, H. J., Min, Y. H., Choi, E. C., Shin, Y. K., Park, B. J., ... & Kim, S. (2005). Human lysyl-tRNA synthetase is secreted to trigger proinflammatory response. *Proceedings of the National Academy of Sciences of the United States of America*, 102(18), 6356-6361.
7. Ahn, Y. H., Park, S., Choi, J. J., Park, B. K., Rhee, K. H., Kang, E., ... & Cho, M. L. (2016). Secreted tryptophanyl-tRNA synthetase as a primary defence system against infection. *Nature microbiology*, 2, 16191.
8. Wakasugi, K., & Schimmel, P. (1999). Two distinct cytokines released from a human aminoacyl-tRNA synthetase. *Science*, 284(5411), 147-151.

9. Park, M. C., Kang, T., Jin, D., Han, J. M., Kim, S. B., Park, Y. J., ... & Yang, X. L. (2012). Secreted human glycyl-tRNA synthetase implicated in defense against ERK-activated tumorigenesis. *Proceedings of the National Academy of Sciences*, 109(11), E640-E647.

10. Mosely, S. I., Prime, J. E., Sainson, R. C., Koopmann, J. O., Wang, D. Y., Greenawalt, D. M., ... & Marcus, D. (2016). Rational selection of syngeneic preclinical tumor models for immunotherapeutic drug discovery. Cancer immunology research, canimm-0114.

11. Lechner, M. G., Karimi, S. S., Barry-Holson, K., Angell, T. E., Murphy, K. A., Church, C. H., ... & Epstein, A. L. (2013). Immunogenicity of murine solid tumor models as a defining feature of in vivo behavior and response to immunotherapy. Journal of immunotherapy (Hagerstown, Md.: 1997), 36(9), 477.

12. Dranoff, G. (2012). Experimental mouse tumour models: what can be learnt about human cancer immunology?. Nature Reviews Immunology, 12(1), 61-66.

13. Lechner, M. G., Karimi, S. S., Barry-Holson, K., Angell, T. E., Murphy, K. A., Church, C. H., ... & Epstein, A. L. (2013). Immunogenicity of murine solid tumor models as a defining feature of in vivo behavior and response to immunotherapy. *Journal of immunotherapy* (Hagerstown, Md.: 1997), 36(9), 477.

14. Ofuji, K., Tada, Y., Yoshikawa, T., Shimomura, M., Yoshimura, M., Saito, K., ... & Nakatsura, T. (2015). A peptide antigen derived from EGFR T790M is immunogenic in non‐small cell lung cancer. *International journal of oncology*, 46(2), 497-504.

15. Oishi, S., & Fujii, N. (2012). Peptide and peptidomimetic ligands for CXC chemokine receptor 4 (CXCR4). *Organic & biomolecular chemistry*, 10(30),

5720-5731.

16. Mantovani, A., Marchesi, F., Malesci, A., Laghi, L., & Allavena, P. (2017). Tumour-associated macrophages as treatment targets in oncology. *Nature reviews Clinical oncology*, 14(7), 399-416.

17. Zaidi, M. R., & Merlino, G. (2011). The two faces of interferon-γ in cancer. Clinical cancer research, 17(19), 6118-6124.

18. Martins, G. R., Gelaleti, G. B., Moschetta, M. G., Maschio-Signorini, L. B., & Zuccari, D. A. P. D. C. (2016). Proinflammatory and Anti-Inflammatory Cytokines Mediated by NF-κB Factor as Prognostic Markers in Mammary Tumors. Mediators of inflammation, 2016.

19. Williams, T. F., Mirando, A. C., Wilkinson, B., Francklyn, C. S., & Lounsbury, K. M. (2013). Secreted Threonyl-tRNA synthetase stimulates endothelial cell migration and angiogenesis. Scientific reports, 3.

20. Chan, S. W., & Egan, P. A. (2005). Hepatitis C virus envelope proteins regulate CHOP via induction of the unfolded protein response. *The FASEB journal*, 19(11), 1510-1512.

21. Villanueva, M. T. (2017). Immunotherapy: Macrophages steal the show. *Nature reviews. Cancer*, 17(7), 396.

22. De Henau, O., Rausch, M., Winkler, D., Campesato, L. F., Liu, C., Cymerman, D. H., ... & Douglas, M. (2016). Overcoming resistance to checkpoint blockade therapy by targeting PI3Kγ in myeloid cells. *Nature*, 539(7629), 443-447.

23. Elgueta, R., Benson, M. J., De Vries, V. C., Wasiuk, A., Guo, Y., & Noelle, R. J. (2009). Molecular mechanism and function of CD40/CD40L engagement in the immune system. *Immunological reviews*, 229(1), 152-172.

요약 (국문초록)

면역 촉진을 통한
Human Cysteinyl-tRNA Synthetase의 항암 활성

서울대학교
융합과학기술대학원
분자의학 및 바이오제약학과 의약생명과학전공
한만규

면역항암치료제는 인체 내 면역체계를 통해 항암효과를 나타내는 것으로 알려져있다. 면역항암치료는 기존 3대 암 치료법인 수술, 항암화학요법, 방사선치료에서 발견된 부작용을 보완한 치료법으로 장점으로는 지속성, 상대적으로 낮은 독성, 그리고 악성종양부터 여러 종류의 종양에 사용가능하다는 점 등이 있다. 아미노아실 tRNA 합성효소(Aminoacyl tRNA synthetases, ARSs)는 아미노산과 tRNA를 연결하는 본래의 기능 이외에도 다양한 기능을 하는 것으로 알려져 있다. 본 연구에서는 시스테이닐 tRNA 합성효소(Cysteinyl-tRNA synthetase, CRS)가 면역을 매개하여 항암효과를 나타냄을 밝혔다. 동종동계이식 동물 모델을 이용한 스크리닝을 통해 CRS의 종양 억제 효과를 확인하였다. 또한 CRS가 선천성 면역체계의 대식세포에 결합하며, 이를 활성화하여 TNF-α 분비를 증가시키고, 대식세포의 이동 및 종양미세환경으로의 침윤을 촉진함으로써 항암효과를 나타내는 것을 시험관 내(*in vitro*) 실험 및 생체 내(*in vivo*) 실험을 통해 확인하였다. 또한

일부 대장암 세포에서 여러 사이토카인 중 TNF-α 및 Tunicamycin (소포체 스트레스) 에 특이적으로 반응하여 CRS가 분비됨을 확인하였다. 결론적으로 본 연구 결과를 통해, 분비된 CRS가 케모카인 또는 염증유발 사이토카인으로 작용함으로써 항암 작용을 매개할 것이라 사료된다.

주요어 : Cysteinyl-tRNA synthetase, 면역항암, 대식세포, TNF-α, 케모카인, 사이토카인

학 번 : 2016-26019